Molecular fractionation in melt-crystallized polyethylene: 1. Differential scanning calorimetry*

U. W. Gedde and J.-F. Jansson
Department of Polymer Technology, The Royal Institute of Technology, S-100 44 Stockholm, Sweden
(Received 1 January 1983; revised 14 May 1983)

This is the first paper in a series in which molecular fractionation (segregation) in melt-crystallized polyethylene (PE) has been studied by differential scanning calorimetry (d.s.c.). A number of PE's (both high- and medium-density materials) have been given a variety of thermal treatments, including isothermal crystallization from the melt and annealing. The melting of the samples as registered by d.s.c. has been extensively analysed and information regarding the crystallization, particularly in relation to molecular fractionation, is presented.

Keywords Melt-crystallized polyethylene; molecular fractionation; crystallization kinetics; melting; molecular structure

INTRODUCTION

Segregation of polymer molecules of different molecular weights into different crystals during crystallization is generally referred to as molecular weight segregation. A more general concept would be molecular fractionation or segregation, applying to the separation during crystallization of molecules different from each other even in other respects than molecular weight. For instance, experimental evidence has been presented for the segregation in polyethylene (PE) of molecules of different degrees of branching[1].

Molecular fractionation is a field in polymer physics that has received some attention during the last decades. Segregation in PE on crystallization from solution was first reported by Richardson[2]. A number of important studies on this topic have been published[1,3-5], but, segregation in melt-crystallized PE only received attention later. Experimental studies providing evidence for segregation in melt-crystallized systems have been reported by a number of authors[6-18]. Wunderlich[19,20] summarized in 1974 the experimental evidence for molecular fractionation and rationalized it in terms of a hypothesis in which a concept introduced by the author, molecular nucleation, played a vital role. According to Wunderlich, at each temperature of crystallization (T_c) there exists a critical molecular weight M_{crit} with the following meaning: molecules of a molecular weight greater than $M_{crit}(T_c)$ are able to crystallize at T_c. However, molecules of a molecular weight less than $M_{crit}(T_c)$ are unable to crystallize at T_c. These molecules may only crystallize on further cooling. To explain this behaviour, Wunderlich introduced the molecular nucleation concept. It applies to the process which establishes the first part of a macromolecule in the crystalline phase. Agreement was obtained between the size of the molecular nucleus, as determined by classical nucleation theory, and the size of the critical species experimentally found. Later Lindenmeyer *et al.*[21] showed that polymer crystallization including molecular fractionation can be described by small system thermodynamics. In addition to the simple temperature dependence of M_{crit} experimentally indicated and explained by the hypothesis of Wunderlich, a dependence on the type of nucleation site was considered. According to this model there exists a M_{crit}–T_c relation for each type of nucleation site. Hence, fractionation should not be absolutely sharp in terms of molecular weight at any given T_c.

In this paper, which is the first in a series concerned with molecular fractionation in PE, extensive studies of melt-crystallized systems by d.s.c. are presented. So far, three reports have considered the melting of linear polyethylene (LPE) in relation to molecular fractionation[12,13,16]. The findings reported in these studies were as follows:

(a) Samples isothermally crystallized (at T) from the melt or isothermally annealed (at T) and then rapidly cooled to room temperature frequently show two melting peaks[12,13]. The high temperature (HT) peak showing superheating[13], here referred to as the non-segregated component, is associated with the melting of the material that has crystallized at T[12,13], whereas the low temperature (LT) peak not showing superheating[13], in this paper referred to as the segregated component, is associated with the melting of material crystallized not at T but during the subsequent cooling at a lower temperature.

(b) It was shown by Mehta and Wunderlich[13] that in samples isothermally crystallized for longer periods than $5 \times t_{0.5}$ ($t_{0.5}$ is the time required for 50% crystallization to occur), the LT peak is composed of low molecular weight material.

(c) The time dependence of crystallization at 127°C was studied by Mehta and Wunderlich[13] on a Rigidex PE. They observed a monotonic decrease in the area under the LT peak for times shorter than 30 h. At longer times, no further change in the LT peak area could be observed. The

* A part of this paper was presented at the 14th Europhysics Conference on Macromolecular Physics, Vilafranca del Penedes, Spain, September 1982

0032-3861/83/121521-11$03.00

Table 1 Polyethylenes investigated

Material code	$\bar{M}_n \times 10^{-3}$ [a]	$\bar{M}_w \times 10^{-3}$ [a]	MI_2 [b]	Density (kg m^{-3})[c]	CH_3/1000 C	
					d	*e*
7022	7.4	51	22	963	2	5.5
7006	8.4	90	7	960	6	7.5
2912	21.6	199	0.3	957	4	9
2215[f]	22.0	286	0.05	953	5	14.5
6375	12.9	108	–	>960	0.6	0.6
3140[g]	12.4	166	0.7	940	16	25

[a] By gel permeation chromatography
[b] Melt flow index according to ISO/R 292
[c] On the material as obtained from the manufacturer according to ASTM D 1505–68
[d] By infrared (i.r.) spectroscopy on solid films. The 1379 cm^{-1} peak (assigned to the methyl groups[22]) was estimated with reference to the 1463 cm^{-1} peak (assigned to the methylene groups[22]), and calibration was carried out by recording the spectrum of liquid straight-chain octadecane
[e] From crystallinity determinations by d.s.c. using literature data[31] relating branching content and crystallinity. The highly linear material 6375 was taken as a reference in these calculations
[f] Material 2215 is a copolymer with butene-1 as the comonomer of a concentration resulting in about one ethyl group per 100 carbons
[g] This material is a 50/50 (wt/wt) blend of linear PE (MI_2 = 0.7 and density = 960 kg m^{-3}) and branched PE (MI_2 = 0.7 and density = 920 kg m^{-3})

authors rationalized these findings in the existence of three types of molecules at 127°C: crystallized larger molecules, uncrystallized molecules which at a later stage may crystallize at 127°C, and rejected low molecular weight species unable to crystallize at 127°C.

(d) Samples of binary mixtures of LPE fractions of $\bar{M}_n$ = 980 and 1790 cooled at a rate of 10 K min^{-1} showed two melting peaks, indicating segregation between the components[16]. However, samples quenched in ice water showed only one melting peak[16]. With confirmatory data by small-angle X-ray scattering the authors concluded that segregation depends on the time available for crystallization, which in that particular study was controlled by the cooling rate[16].

EXPERIMENTAL

Materials

The polyethylenes studied were characterized as described in *Table 1*. The methyl group concentration determined by i.r. spectroscopy is somewhat incorrect as the methyl groups included in the crystals are not included in this analysis[22]. An alternative method was applied therefore as shown in *Table 1*. Particularly for sample 2215 the latter method gave a value more consistent with that obtained from the polymerization conditions.

Preparation of samples

Heat treatment was carried out both in the d.s.c. apparatus (temperature correct within 0.1K) and in a constant temperature bath (recording better than 0.1K, temperature variation with time ±0.15K). The 5 mg samples were treated in the d.s.c. in a nitrogen atmosphere to avoid thermal oxidation. The more time-consuming treatments were carried out in the constant temperature bath with the samples sealed in vacuum in glass tubes.

A standard crystallization procedure, cooling at a constant rate from above the melting point, was carried out occasionally to detect undesired changes in the heat-treated samples. D.s.c. scans were then recorded from 300 to 450K and in no case were changes in these curves detectable.

The samples were treated in two different ways:

(1) Isothermal crystallization (IC) from the melt (450K) at a temperature T_c for different times t_c. The systems were finally cooled to room temperature at either 1.25 K min^{-1} or 80 K min^{-1}. The crystallization was truly isothermal for treatments carried out in the d.s.c. and for most of the treatments carried out in the constant temperature bath. However, for treatments of T_c equal to 393.2K, the constant temperature bath crystallization starts within the temperature range 394–395K.

(2) Annealing (A) at a temperature T_a for different times t_a of systems originally crystallized at a cooling rate of 1.25 K min^{-1} (crystallization is initiated at ~396K and the crystallization rate is at a maximum between 394–394.5K at this cooling rate) from the melt (450K). After the annealing phase, the samples were cooled to room temperature at a rate of 1.25K min^{-1}.

Differential scanning calorimetry (d.s.c.)

The d.s.c. instrument, a Perkin-Elmer DSC-2 was calibrated at a scan rate of 10K min^{-1} according to standard procedures with an accuracy better than 0.1K. The instrumental base line between 300 and 450K was regularly controlled and held straight. The melting endotherms were normally recorded at 10K min^{-1}. The instrument was recalibrated when other scan rates were used.

The experimental procedures to obtain d.s.c. temperatures to an accuracy of 0.1K have been discussed by several authors[24–26]. The conditions for obtaining such an accuracy were fulfilled in the present study. The melting endotherms presented in this report are all corrected (by a computer) for the thermal lag between the sample pan and the sample holder in accordance with ref. 25. The thermal resistance was determined from melting data of highly pure indium.

With the aid of a digitizer, the melting endotherms were analysed by taking 60–80 points along each curve. A computer program made it possible to transform these points into melting energies, etc.

Choice of base line

The choice of a proper base line with reference to melting of PE has been discussed by several authors, e.g.

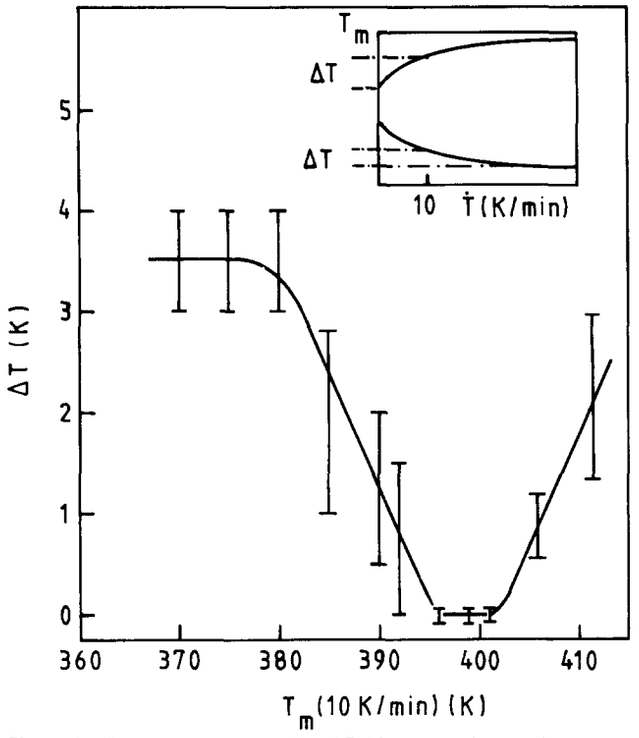

Figure 1 Temperature correction ΔT (determined according to the small figure) as a function of melting point recorded at 10 K min^{-1} heating rate (T_m(10 K min^{-1})). A few data from the literature[13,32] are included

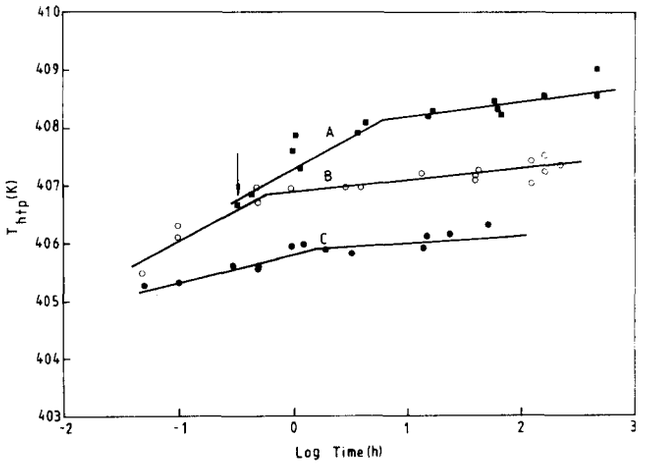

Figure 2 Melting peak temperature (T_{htp}) plotted *versus* the logarithm of the crystallization time (t_c). The samples, all 6375, were crystallized from the melt at A, 401 K; B, 398.2 K; and C, 393.2 K for different times t_c. The arrows indicate the start of crystallization at the respective T_c's

Gray[27], Richardson[28] and Blundell *et al.*[29] One of the methods suggested, the total enthalpy method, was chosen because the base line obtained by this method crosses the $dH/dt - T$ curve at the onset of non-rectilinearity of this curve. Thus, this base line choice is consistent with the appearance of the base line constructed from the specific heat data by Wunderlich and Baur[30]. All crystallinity determinations are based on a value of 293 kJ kg^{-1} as the heat of fusion of 100% crystalline PE[31].

Dependence of melting on heating rate

The path of melting of polymer crystals is related to heating rate, as has been discussed by Wunderlich[31]. Imperfect and small crystals rearrange on heating so that they finally melt at a higher temperature than if not rearranged. With slower heating this effect is more pronounced. Large crystals having a higher melting point show superheating which is minimized as the heating rate approaches zero. Melting of crystals of intermediate melting point are independent of heating rate. By running d.s.c. scans at different rates from 0.6 to 160K min^{-1} on PE samples crystallized in a specific manner (80K min^{-1} cooling from the melt), all three types of behaviour could be observed in the polycrystalline samples (*Figure 1*). The melting peak temperatures were also recorded for another 16 samples at different scan rates giving additional ΔT data in the high temperature region of *Figure 1*. The temperature correction term ΔT refers to the melting path at 10K min^{-1}. If ΔT is subtracted from T_m (10K min^{-1}), a melting temperature is obtained which is corrected for the effect of rearrangement and superheating. The melting endotherms presented in this report are all treated according to this procedure with the aid of a computer program.

RESULTS AND DISCUSSION

The high temperature (HT) peak

The relations between the peak temperature (T_{htp}) and the crystallization time (IC treatment) is shown in *Figure 2*. All the data obtained follow essentially rectilinear relations with two different slopes. At short times, T_{htp} increases markedly with increasing crystallization time (stage 1 crystallization), whereas later a less marked increase in T_{htp} is observed (stage 2 crystallization). Similar results have been reported by Weeks[33] and by Dlugosz *et al.*[14] The latter authors suggested that the mechanism of Kawai[34] should be partly responsible for the crystal thickening of stage 1.

According to Kawai[34], the higher molecular weight species start to crystallize giving rise to comparatively thin crystals. With time, the lower molecular weight material starts to crystallize at a lower degree of supercooling, resulting in the formation of thicker crystals. In stage 2, 'true' isothermal thickening, older crystals growing in the chain axis direction, should instead be responsible, as suggested by Hoffman and Weeks[35]. Values of the slopes of the stage 1 and 2 crystallizations are presented in *Table 2*.

The stage 1 changes in T_{htp} with crystallization time at 398.2 and 401.2K are approximately the same for all the samples, between 0.9 and 1.5K $decade^{-1}$. At 393.2K, crystallization starts so rapidly that a major part of the stage 1 crystallization is outside the experimental range. The data obtained are in agreement with dilatometric data of Weeks[33]. He defined the melting point as the temperature where 0.01 of original crystallinity exists on heating at 0.18K min^{-1}. Weeks[33] obtained a value for the stage 1 slope of 1.4K $decade^{-1}$ for crystallization temperatures between 398.2 and 403.2K.

The scatter of the data of the stage 2 crystallization is larger. At 393.2K, T_{htp} increases at $\leqslant$0.1K $decade^{-1}$. At 398.2K, it increases between 0.1 and 0.4K $decade^{-1}$, and at 401.2K the increase is between 0.2 and 0.5K $decade^{-1}$. Weeks[33] obtained the following values from dilatometric data: 393.2K, 0.05K $decade^{-1}$; 398.2K, 0.2K $decade^{-1}$; 401.2K, 0.4K $decade^{-1}$. Dlugosz *et al.*[14] observed by Raman spectroscopy on a LPE crystallized at 399.2K a

Table 2 Data of the HT peak of samples isothermally crystallized from the melt

Material	Temperature (K)	$dT_{htp}/d\log t$ (K/log h)		$T_{htp,i}$ (K)
		stage 1	stage 2	
7022	393.2	–[a]	0.1	<403.6
7022	398.2	1.3	0.05	404.5
7022	401.2	0.9	0.2	407.2
7006	393.2	–[a]	0.05	<404.0
7006	398.2	1.1	0.15	404.9
7006	401.2	1.3	0.35	406.7
2912	393.2	–[a]	0.1	<405
2912	398.2	1.1	0.4	405.9
2912	401.2	1.2	0.5	407.2
2215	393.2	–[a]	0.4	<403.7
2215	398.2	1.3	0.4	405.1
2215	401.2	1.1	–	407.0
3140	393.2	–[a]	–	<403
3140	398.2	0.9	0.2	404.7
3140	401.2	0.9	0.3	406.6
6375	393.2	–[a]	0.1	<405
6375	398.2	1.0	0.2	<405.5
6375	401.2	1.1	0.25	406.8

[a] Outside the experimental range

thickness growth of 2.5 nm decade^{-1} which corresponds to an increase in melting point of 0.3K decade^{-1}. In conflict with these data stand recent findings by Varnell *et al.*[36] They found no evidence for isothermal thickening (stage 2) in studies of LPE samples by SAXS or d.s.c.

The melting point of the first-formed crystals ($T_{htp,i}$) depends primarily on the temperature of crystallization which is most evident from *Table 2*. By applying an equation according to Hoffman[39], $T_m = T_m^0(1-1/\gamma)+T_c/\gamma$, where T_m is the melting point of a crystal grown at T_c, γ is a constant and T_m^0 is the equilibrium melting point, to the data for T_c equal to 398.2K and 401.2K, a value of 402K is obtained for $T_{htp,i}$ at $T_c = 393.2$K. An extrapolation of the data to $T_m = T_c$ gives $T_m^0 = 415$K. Applying the data of Illers and Hendus[37], thickness data for the first-formed crystals can be estimated: 393.2K—less than 24.5 nm (24.3 nm), 398.2K—26.8–29.9 nm (27.3 nm), 401.2K—34.0–37.1 nm (27.9 nm). The values within brackets are from a recent study by Barham *et al.*[38]

Detailed study of the changes of the HT peak as a function of crystallization time

Changes within the HT peak in a system of invariant value of the fraction of segregated component (W_s), i.e. of LT peak material, were studied on sample 6375 isothermally crystallized from the melt at 398.2K. The weight fraction of crystalline segregared component $W_{s,c}$ (mass fraction of crystalline segregated component $W_{s,c}$ (mass almost constant over 2.5 decades in crystallization time, *Figure 3*. From the same Figure, it is evident that the crystallinity increases during the same period of time.

As the content of segregated component is constant, the increase in crystallinity (2.5% per decade) must be assigned to a transformation of the amorphous material associated with the crystalline regions, presumably interlamellar amorphous material, to crystalline material. The increase of the crystalline regions amounts to $0.025/W_{ns,c} = 0.035$ per decade. Using the melting point—crystal thickness data of Illers and Hendus[37] and assuming that the crystal growth (3.5% per decade) occurs along the chain axis, which is reasonable on the basis of surface energy data, this increase in crystal thickness would amount to 1.3 nm decade^{-1}. Here, the melting point data, transformed into crystal thickness by the data of Illers and Hendus[37], reveals an increase of 1.5 nm decade^{-1}.

Figure 4 shows the development of the HT peak with crystallization time in more detail. These data are clearly consistent with a 'true' isothermal crystal thickening to be identified with the stage 2 crystallization.

Samples 7006 and 7022 isothermally crystallized at 401.2K have been used as model materials to study changes within the HT peak for systems of changing W_s. The model used in the calculations is presented in *Figure 5*.

The changes with crystallization time of mass fractions of the three systems (crystals melting between 406–408K, 408–410K and 410–412K, respectively) are calculated from the melting endotherms. To solve this system of

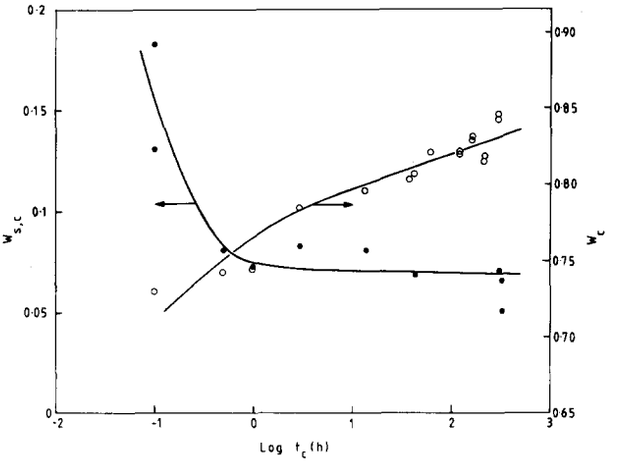

Figure 3 Mass fraction of the sample melting within the LT peak ($W_{s,c}$) and the crystallinity (W_c) at 300 K plotted *versus* the logarithm of crystallization time (t_c) of samples (6375) crystallized from the melt at 398.2 K for different times t_c and then cooled to 300 K at a rate of 80 K min^{-1}

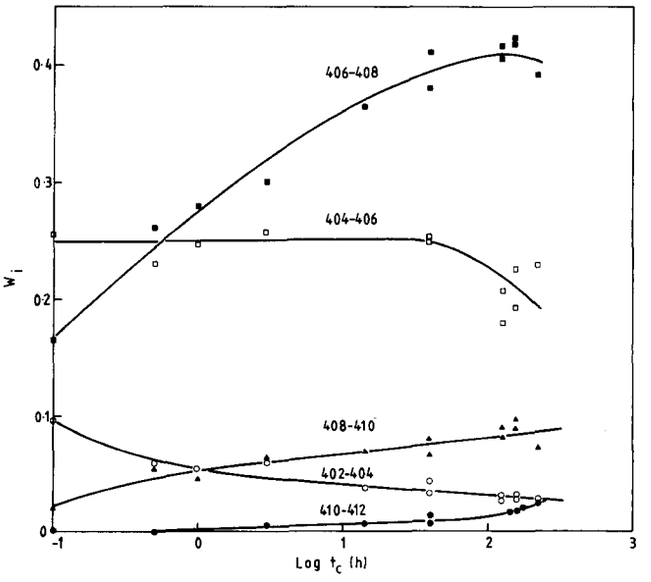

Figure 4 Mass fraction (W_i) of the sample that is melting within the temperatures: ■, 406–408; □, 404–406; ▲, 408–410; ○, 402–404; ●, 410–412 K plotted *versus* the logarithm of the crystallization time (t_c) for samples of 6375 crystallized from the melt at 398.2 K for different times

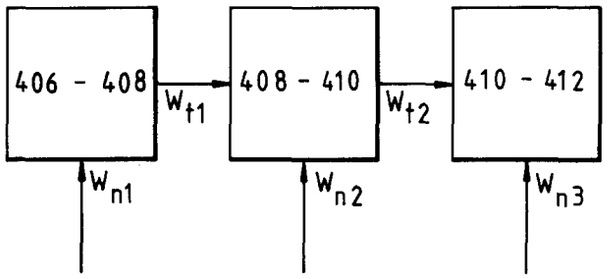

Figure 5 Model used for the calculation of the rate of formation of new crystals (W_{n1}, W_{n2} and W_{n3}) and the rate associated with the 'true' isothermal thickening (W_{t1} and W_{t2})

Table 3 Results fromthe calculations of the crystal thickening components

Sample[a]	Time interval (h)	W_{t1} (%)	W_{t2} (%)	W_{n1} (%)	W_{n2} (%)	W_{n3} (%)
7006	5 –16.5	1.2	0.5	10.2	6.8	0.7
7006	16.5–87	2.4	1.7	5.7	4.7	0.1
7006	87 –115	0.4	0.3	0.4	0	0
7022	5 –16.5	0.3	0.2	9.5	5.8	0
7022	16.5–40	0.5	0.4	3.2	5.6	1.3
7022	40 –88	0.5	0.6	0	5.9	1.5

[a] The samples were crystallized from the melt at 401.2 K for different times

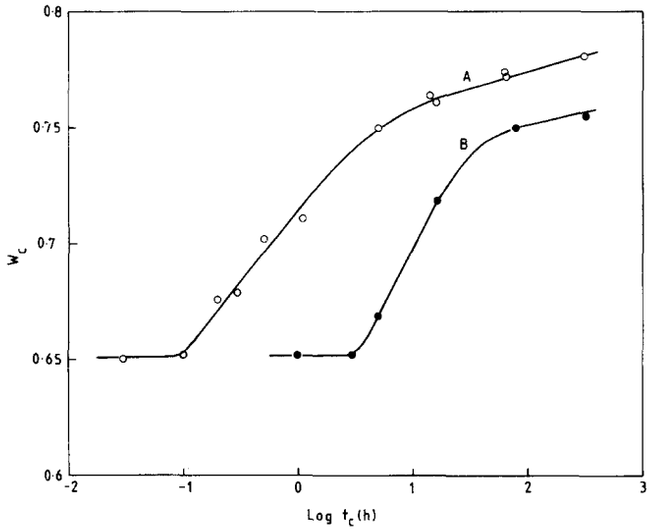

Figure 6 Crystallinity (W_c) at 300 K as a function of the logarithm of the crystallization time (t_c) for samples of 7006 crystallized from the melt at A, 398.2 K; and B, 401.2 K for different times t_c. The samples were finally cooled at a rate of 80 K min^{-1} to 300 K

equations (five unknown and three independent equations), W_{t1} and W_{t2} are estimated on the basis of the growth rate prevailing during stage 2. Thus, it is assumed that the melting points of the crystals of the systems are shifted, on an average, 0.35 (7006) and 0.2 (7022) K decade^{-1}, respectively. The flow (for 7006) from one system into the adjacent equals $0.35 \cdot (\log t_{end} - \log t_{start}) \cdot W_i/2$. *Table 3* presents the result of these calculations.

The data in *Table 3* indicate that the rapid shift of the HT peak in stage 1 is primarily due to the fact that the newly crystallized molecules form with time crystals of increasingly higher melting points. This statement is based on the observation that W_{n2} and W_{n3} decrease more slowly with crystallization time than W_{n1}.

Relations between crystallinity and fraction of segregated component

Typical plots showing how the crystallinity (after cooling to 300K, as obtained by d.s.c.) of samples crystallized isothermally from the melt for different times, relates to crystallization time are presented in *Figure 6*.

Three zones can be distinguished in the plots of *Figure 6*. At short times, before initiation of crystallization occurs at T_c, a region of constant crystallinity (W_c) is observed. At intermediate times, a region of rapidly increasing W_c is apparent, corresponding to the phase of rapid crystallization at T_c, i.e. the stage 1 crystallization. At long times, a region of slowly increasing W_c is observed which corresponds to the stage 2 crystallization. Thus, the increase in W_c is a consequence of the increasing crystallinity of the semicrystalline non-segregated component. From this discussion it seems reasonable to assume that W_c and W_s should be related. *Figure 7* plots these quantities and gives the definitions of crystallinities of the segregated and the non-segregated components. The problem in using equation (1) to calculate $W^0_{s,c}$ and $W^0_{ns,c}$ is that to obtain W_s and W_{ns}, $W^0_{s,c}$ and $W^0_{ns,c}$ have to be known. To solve this problem, W_c was plotted *versus* $W'_s = W_{s,c}/(W_{s,c} + W_{ns,c})$, i.e. the relative size of the LT peak, and approximate values of $W^0_{s,c}$ and $W^0_{ns,c}$ could be estimated. From these new data another group of W_s data was calculated which gave a new $W_c - W_s$ plot and new correct values for W^0_{sc} and $W^0_{ns,c}$. The data shown in *Figure 7* are corrected in this way.

The general appearance of all the plots of the samples studied is rectilinear region covering most of the W_s range and a non-rectilinear region in a limited W_s range. It is apparent that W_c increases in the region where W_s is approximately constant (stage 2 crystallization), i.e. $W^0_{ns,c}$ is changing as a function of time. This is the reason for the non-rectilinearity of the $W_c - W_s$ plot. For the sample

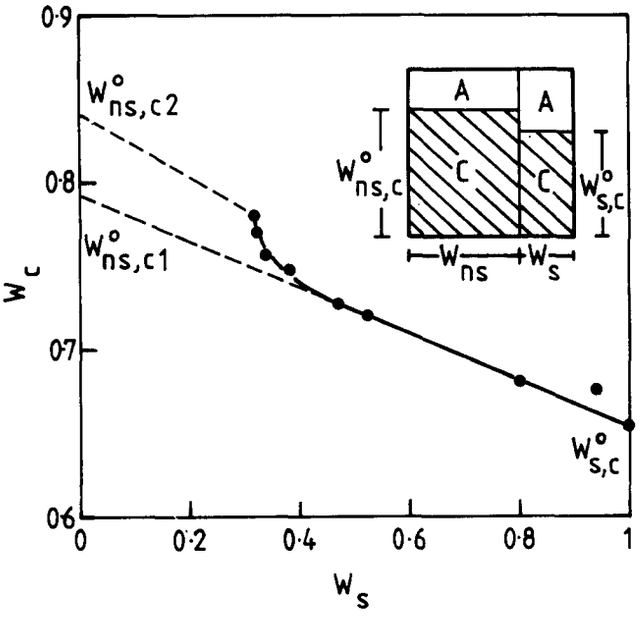

Figure 7 Crystallinity (W_c) at 300 K plotted *versus* the mass fraction of segregated component (W_s) of samples of 7006 crystallized from the melt at 398.2 K for different times t_c. The samples were finally cooled at a rate of 80 K min^{-1}. Each component is considered to have a certain crystallinity, $W^o_{s,c}$ and $W^o_{ns,c}$ respectively (illustrated by the small figure), related to the overall crystallinity according to equation (1):

$$W_c = W_s \cdot W^o_{s,c} + W_{ns} \cdot W^o_{ns,c} \quad (1)$$

Table 4 Crystallinities of segregated and non-segregated components

Material	Cryst. temp.[a] (K)	$W^0_{s,c}$	$W^0_{ns,c1}$	$W^0_{ns,c2}$
7022	398.2	0.65	0.78	0.82
7022	401.2	0.65	0.81	0.84
7006	398.2	0.65	0.79	0.84
7006	401.2	0.65	0.81	0.84
2912	398.2	0.60	0.73	0.79
2912	401.2	0.60	0.77	0.81
2215	398.2	0.575	0.70	0.75
6375	401.2	0.70	0.81	0.87

[a] The samples were cooled from the crystallization temperature to 300 K at a rate of 80 K min^{-1}

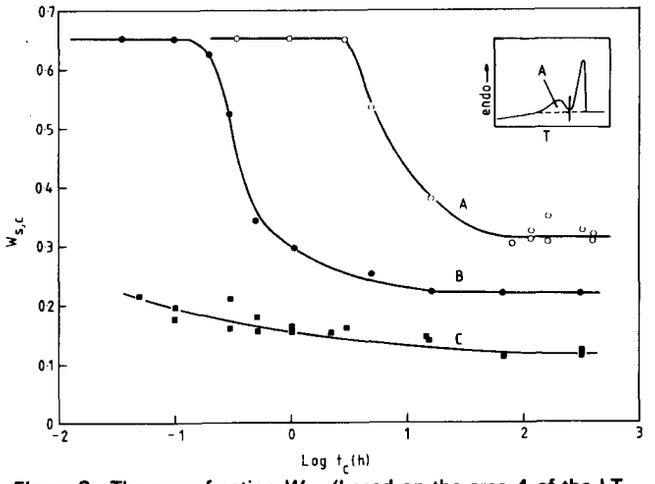

Figure 8 The mass fraction $W_{s,c}$ (based on the area *A* of the LT peak) plotted *versus* the logarithm of the crystallization time (t_c) for different samples: A, 7006, IC-treated at 401.2 K; B, 7006, IC-treated at 398.2 K; C, 2215, IC-treated at 393.2 K. The samples were finally cooled at a rate of 80 K min^{-1} to 300 K

shown in *Figure 7*, $W^0_{ns,c}$ increases from $W^0_{ns,c1}=0.79$ to $W^0_{ns,c2}=0.84$. The rectilinearity of the 0.4–1.0 (W_s) range can be explained by the fact that this change in W_s requires only 0.5 decade of time. The change in $W^0_{ns,c}$ during this period is very limited. *Table 4* presents a summary of the results concerning all the samples studied.

It is clear from the data in *Table 4* that $W^0_{ns,c}$ values are higher at 401.2K than at 398.2K. Comparison with the data of *Table 1* shows that the crystallinity values (both $W^0_{s,c}$ and $W^0_{ns,c}$) decrease with increasing degree of chain branching.

The low temperature (LT) melting peak

Figure 8 shows typical plots of the mass fraction of crystalline segregated component $W_{s,c}$ *versus* $\log t_c$.

An induction period, with no crystallization at T_c (outside the range of curve *C*) where $W_{s,c}$ is constant, is observed at short t_c. It is followed by a phase of decreasing $W_{s,c}$ associated with a period involving the introduction of an increasing number of molecules into the crystalline phase at T_c. Finally, a constant value of $W_{s,c}$ is approached, which correspond to the fraction of the sample unable to crystallize at T_c, regardless of the time. These molecules require a larger degree of super-cooling to crystallize. The constant value approached is denoted $W_{sl,c}$ and the corresponding value relating to the total amount of segregated component (both crystalline and amorphous) is denoted W_{sl}. These results are in principle in agreement with data relating the relative size of the LT peak to t_c reported earlier[12–15]. However, as the area under the HT peak increases with increasing t_c even after the establishment of a constant value of $W_{s,c}$, a slow decrease in the relative size of the LT peak would appear in such a plot. This is avoided by taking $W_{s,c}$ as the judging parameter.

Table 5 presents data for the kinetics of crystallization judged from plots of $W_{s,c}$ *versus* $\log t_c$. It is evident that the regions of isothermal crystallization (between t_{st} and t_e) are shifted to longer times with increasing T_c. Significant differences in t_{st} and t_e are observed for the different materials at the same T_c. The materials ranked in the order of decreasing values in these parameters are as follows: 2215, 2912 = 7006 = 7022, 3140, 6375. The time span, *D*, decreases with increasing T_c: 393.2K – *D* is larger than 2.5 decades (only one value), 398.2K – $D = 1.73 \pm 0.13$, and 401.2K – $D = 1.52 \pm 0.09$. Note the more extended regions of slowly decreasing $W_{s,c}$ at the lower T_c's (*Figure 8*). The existence of this difference in size of the region of slow $W_{s,c}$ is the main reason for the difference in the *D* values. Finally, there seem to be no significant differences between the different materials with regard to the *D* values.

A determination of W_s (W_{sl}) should consider the lower crystallinity of the segregated component and the contribution to the LT peak of the surface melting of the thicker crystals which mainly melt in the HT peak. The former is considered by the application of $W^0_{s,c}$. The increase in W_{sl} taking this into consideration, compared with the value obtained by measuring this quantity as the relative size of the LT peak, ranges from 0.01–0.07 (absolute mass fraction). The contribution from the surface melting should be relatively small, of the order of 0.01–0.02 (absolute mass fraction) of $W_{sl,c}$[41].

Figure 9 shows the development of the peak temperature T_{ltp} with $\log t_c$ for one of the samples. The same three stages as earlier quoted for the $W_{s,c}$ *versus* $\log t_c$ plot appear at the same values of t_c. The decrease in T_{ltp} is due to the fact that the species which crystallize first during the post-isothermal cooling, forming crystals melting in the high temperature region of the LT peak, also have the greatest tendency of the molecules of the LT peak to crystallize at T_c. The following values for T_{ltp} were obtained for the samples treated at the different T_c's and finally cooled at 1.25 or 80K min^{-1} (values within brac-

Table 5 Kinetics of isothermally crystallized samples

Material	Cryst. temp. (K)	log t_{st} (h)	log t_{e1} (h)	log t_{e2} (h)	*D*
7022	393.2	<–1.5	–0.9	0	>1.5
7022	398.2	–0.5	0.85	1.0	1.5
7022	401.2	0.55	1.9	2.0	1.45
7006	393.2	<–1.5	–0.75	–0.25	>1.25
7006	398.2	–0.8	0.75	1.0	1.8
7006	401.2	0.5	1.8	1.9	1.4
2912	393.2	<–1.5	–0.7	0	>1.5
2912	398.2	–0.8	0.75	1.0	1.8
2912	401.2	0.4	1.85	1.95	1.55
2215	393.2	<–1.5	0.5	1.0	>2.5
2215	398.2	–0.3	1.3	1.45	1.75
2215	401.2	1.0	–	–	–
6375	393.2	<–1.5	–1.2	–1.0	>0.5
6375	398.2	<–1.5	–0.3	0	>1.5
6375	401.2	–0.7	0.8	0.9	1.6

Definitions: t_{st} is the time for the onset of isothermal crystallization, t_{e1} is the time at which $W_{s,c}$ deviates by 0.02 from $W_{sl,c}$, t_{e2} is the time at which $W_{s,c}$ deviates by 0.01 from $W_{sl,c}$, and *D* equals the difference between log t_{e2} and log t_{st}

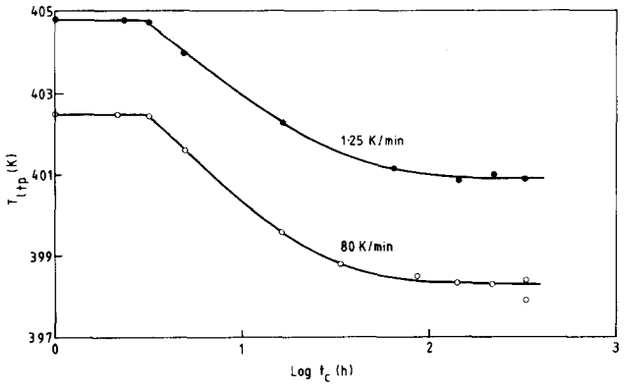

Figure 9 Temperature of the LT peak maximum (T_{ltp}) plotted *versus* the logarithm of the crystallization time (t_c) of samples of 7006 crystallized from the melt at 401.2 K. The samples were cooled after the isothermal treatment at two different rates: ●, 1.25; and ○, 80 K min^{-1}

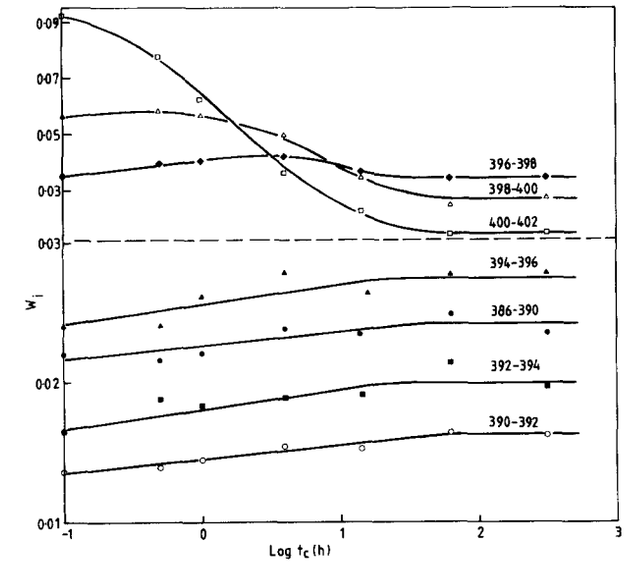

Figure 10 Mass fraction (W_i) of the sample melting within the temperatures: ◆, 396–398; △, 398–400; □, 400–402; ▲, 394–396; ●, 386–390; ■, 392–394; ○, 390–392 K plotted *versus* the logarithm of the crystallization time (t_c) of samples of 7006 crystallized from the melt at 398.2 K. After the isothermal treatment the samples were cooled at a rate of 1.25 K min^{-1} to 300 K

kets): T_c = 393.2K–387.5K (387K), T_c = 398.2K–397.5K (395.5K), T_c = 401.2K–401.0K (398.0K). Thus, it appears that the dependence of T_{ltp} on the final cooling rate increases with increasing T_c.

Figure 10 provides detailed information concerning the development of the LT peak as a function of t_c and the following features are evident:

(1) The high temperature region (400–402K) is gradually suppressed with increasing t_c until finally a constant value is approached. A considerable part of this fraction (present after short crystallization times) will crystallize at T_c on prolonged isothermal treatment. This is also reflected in the gradual decrease of T_{ltp} with increasing t_c as shown in *Figure 9*.

(2) Between 386–394K, however, the W_i's increase with increasing t_c until constant values are approached. This can be explained on the basis of a co-crystallization occurring at low t_c, during the cooling stage, involving molecules of low crystallizability and molecules of a somewhat greater tendency to crystallize. In the case of perfectly linear molecules, these differences in crystallizability can be assigned to differences in molecular weight. On prolonged crystallization at T_c, the latter molecules crystallize and the remaining uncrystallized species of low crystallizability, crystallize on subsequent cooling at lower temperatures than if co-crystallization between the different molecules had occurred. The melting points are shifted correspondingly, in the present case from above 394K to below this temperature.

(3) The fraction melting between 396 and 400K goes through a maximum at short t_c's, decreases and finally approaches a constant value. This is due to a dominance of the process described in (2) at the short t_c's, whereas on prolonged isothermal treatment the process of (1) is of major importance.

(4) The low temperature region, below 386K, is not significantly affected by changes in t_c.

Observations relating to molecular fractionation on crystallization at constant cooling rates

Here, the manner in which the melting endotherms of the samples (7022) treated in the different ways shown in *Figure 11* (treatment type 1, treatment type 2 of various cooling rates $\dot{T}$) relate to each other is considered. It has been shown previously that the LT peak is invariant after approximately 10 h crystallization at 398.2K. All the subsequent comparisons refer to systems having a LT peak of equilibrium size.

Curve A of *Figure 12* refers to the systems obtained after the original cooling from the melt, at different rates. As expected, the fraction of the sample of melting point < 398.2K increases with increasing cooling rate. After 0.1 h annealing at 398.2K, W_s' is almost independent of $\dot{T}$ and after 12–16 h annealing it decreases with increasing $\dot{T}$. The crystallinity of the systems of different $\dot{T}$ annealed for 12–16 h are almost independent of $\dot{T}$. Hence, the decrease in the relative LT peak size for these systems is due to a decrease in the absolute size of the LT peak.

The W_s' value for the treatment 1 system is 0.32 whereas, as shown in *Figure 12*, the values for the treatment 2 systems are considerably lower. This discrepancy in the

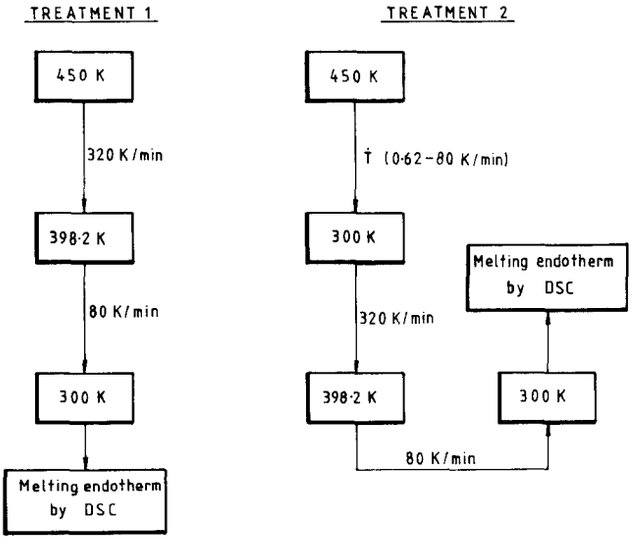

Figure 11 Heat treatments type 1 and type 2. The treatments were carried out in the d.s.c. apparatus. Note that the rate $\dot{T}$ of the initial cooling step of treatment 2 was varied between 0.62 and 80 K min^{-1}

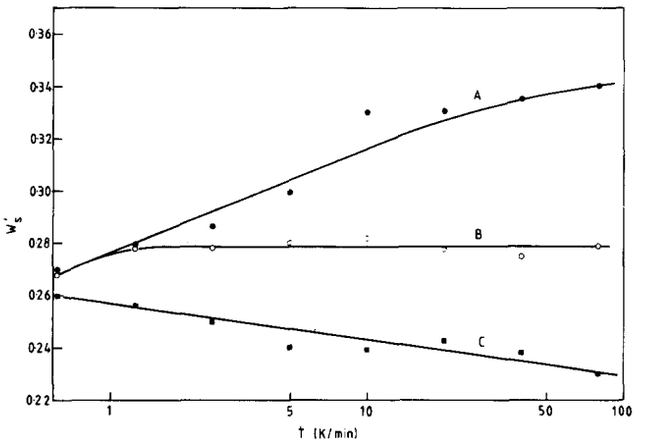

Figure 12 The relative size of the LT peak (W_s') of the treatment 2 systems as a function of the initial cooling rate $\dot{T}$ (logarithmic scale). A, As obtained after the initial cooling. W_s' is defined as the fraction of the sample melting below 398.2 K; B, as obtained after 0.1 h of annealing at 398.2 K; C, as obtained after ≈15 h of annealing at 398.2 K

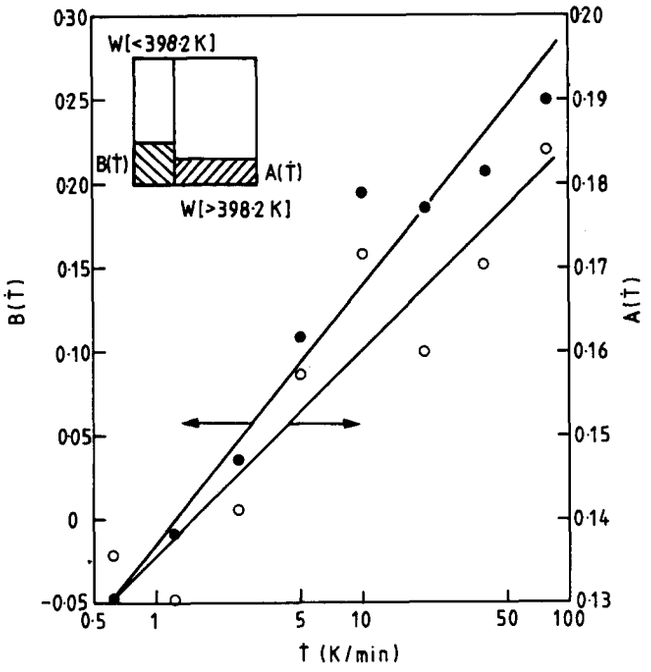

Figure 13 The quantities $A(\dot{T})$ and $B(\dot{T})$ plotted *versus* the initial cooling rate $\dot{T}$ (logarithmic scale). The meaning of these quantities, illustrated by the small figure is described in the text. The precise calculation of $A(\dot{T})$ and $B(\dot{T})$ is as follows:

$$A(\dot{T}) = ((W_{c1}/W^{\circ}_{s,c} W_{s1}' - (W_{c2}/W^{\circ}_{s,c}) W_{s2}'(\dot{T}))/W(T > 398.2\text{ K})(\dot{T})$$
$$B(\dot{T}) = (W(<398.2\text{ K})\ (\dot{T}) - W_{s2}'\ (\dot{T}) \times (W_{c2}/W^{\circ}_{s,c}))/W(<398.2\text{ K})\ (\dot{T})$$

where $W(<398.2\text{ K})$ and $W(>398.2\text{ K})$ are associated with the fractions of the sample melting below and above 398.2 K, respectively (in the systems as obtained after the initial cooling step of treatment 2), W_{s1}' and W_{s2}' are the relative size of the LT peak for samples treated according to 1 or 2, W_{c1} and W_{c2} are the crystallinities for the treatment 1 and treatment 2 systems (15 h of annealing), respectively

W_s' is due to the fact that a fraction of the species, not crystallizable at 398.2K by treatment 1, is included in the crystals of melting point > 398.2K in the systems obtained after the initial cooling phase of treatment 2.

The quantity $A(\dot{T})$ refers to the fraction of uncrystallizable material (by treatment 1, at 398.2K) which has been included in crystals of melting point > 398.2K in the systems obtained after the initial cooling step of treatment 2, whereas $B(\dot{T})$ is the fraction of the crystallizable material (by treatment 1, at 398.2K) which is included in crystals of melting point < 398.2K in the systems obtained after the initial cooling phase of treatment 2. Both $A(\dot{T})$ and $B(\dot{T})$ are defined in *Figure 13*. The equations presented consider the differences in crystallinity of the components using the data of *Table 4*.

Figure 13 shows that both $A(\dot{T})$ and $B(\dot{T})$ increase with increasing cooling rate $\dot{T}$. This indicates that: (a) crystals melting at > 398.2K are contaminated with less crystallizable species (segregated material by treatment 1) to a greater extent in the rapidly cooled systems than in the slowly cooled ones; and (b) crystals melting at < 398.2K contain more of the highly crystallizable material (non-segregated material by treatment 1) in the rapidly cooled systems than in the slowly cooled systems.

The following conclusions are derived from *Figures 14–16* regarding the changes of the LT peak as a function of thermal history:

(1) The reduction of W_s' with increasing $\dot{T}$ is a consequence of the progressive reduction in the high temperature region with increasing $\dot{T}$. This effect is also reflected in the monotonic decrease in T_{ltp} with increasing $\dot{T}$.

(2) A smaller but still significant increase is observed in the low temperature region with increasing $\dot{T}$.

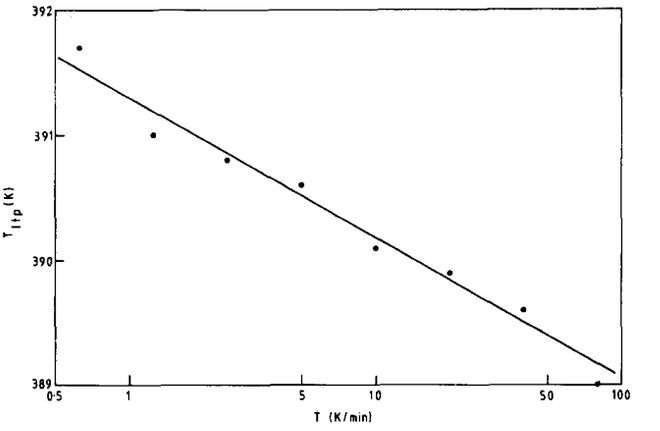

Figure 14 The LT peak temperature (T_{ltp}) plotted *versus* the initial cooling rate $\dot{T}$ (logarithmic scale) for the treatment 2 samples annealed at 398.2 K for 15 h

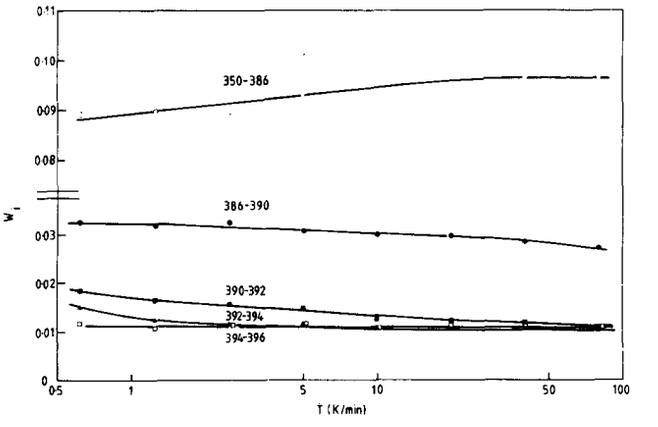

Figure 15 LT peak shape (mass fraction W_i melting within the temperatures: ○, 350–386; ●, 386–390; ■, 390–392; ▲, 392–394; □, 394–396 K) of the treatment 2 systems at 398.2 K for 15 h as a function of the initial cooling rate $\dot{T}$

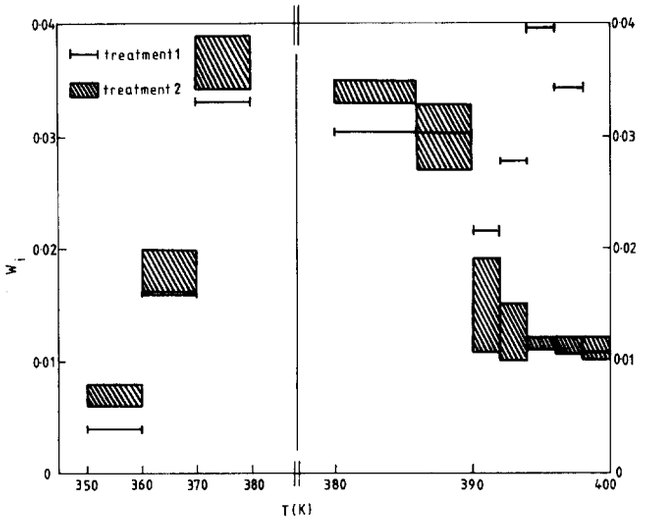

Figure 16 Comparison between the treatment 1 and the treatment 2 systems focussing on the LT peak shape. The scattering of the latter is due to the variation of the initial cooling rate $\dot{T}$. The mass fraction of the samples melting within the temperature ranges indicated are presented

(3) The higher W_s' value of the treatment 1 system compared with those of the treatment 2 systems is reflected in the reduced high temperature region of the treatment 2 systems. The low temperature region, however, is slightly more developed in the treatment 2 systems.

A system of the type investigated here should be considered as a multicomponent system having a distribution of chain defects for the ensemble of molecules. The defects can in principle be of different types: chain ends, chain branches, segments of unsaturation, etc. The number of defects and their severity in a molecule will determine its ability to crystallize at a certain temperature. In LPE systems the chain ends are of major importance and consequently molecular weight segregation has been observed[2-20]. In the ideal case, each component with a certain ability to crystallize should crystallize separately. In reality, the molecules will not crystallize in this simple way. Some co-crystallization between different kinds of molecules, mainly between those of the molecules which are rather similar, will occur. A more complex relation between the distribution in molecular structure of the ensemble of molecules and the crystallization (melting) point distribution, also involving factors such as cooling rate, applies to such a system. This is, of course, the extended conclusion of the data shown in *Figures 12–16*.

A consequence of this discussion is the observed reduction in the high temperature region of the LT peak with increasing $\dot{T}$ for the treatment 2 systems. The molecules which are almost crystallizable at 398.2K (by treatment 1), have a relatively high tendency to crystallize forming crystals of a melting point just less than 398.2K in the slowly cooled treatment 2 systems. However, in the rapidly cooled systems, these species show an increased tendency to co-crystallize with more easily crystallizable molecules and form crystals with a melting point >398.2K. The pronounced difference between the treatment 1 and the treatment 2 systems regarding the W_s' values and the high temperature region of the LT peak indicate that, even at the lowest cooling rate studied, a certain amount of co-crystallization occurs. This co-crystallization has another observable effect on the LT peak of the treatment 2 systems (item 3 above) due to the following reason: The solidification of the LT peak material, which occurs during the final cooling stage, involves less co-crystallization between molecules almost crystallizable at 398.2K (by treatment 1) and molecules of somewhat lower tendency to crystallize in the treatment 2 systems of high $\dot{T}$ than in e.g. the treatment 2 systems of low $\dot{T}$. The crystallization point distribution and hence the melting point distribution are shifted, as observed, towards lower temperatures for the treatment 2 systems of high $\dot{T}$ (compared with the other systems).

Earlier studies by Smith and St. John-Manley[16] on binary mixtures of long-chain straight-chain alkanes have shown that segregation of the components into different crystals is dependent on the time available (cooling rate) during the solidification. The present study shows that this finding also applies to systems such as high-density PE with a continuous molecular weight distribution. A method for the quantification of the degree of co-crystallization of molecules having different tendencies to crystallize has been developed. The quantities, $A(\dot{T})$ and $B(\dot{T})$ obtained by this method provide information concerning the segregation of systems crystallized during constant rate cooling.

The effect of annealing (A) on the melting behaviour—a comparison with the melting behaviour of samples isothermally crystallized from the melt (IC)

The aim of these studies was to study the differences and the similarities in melting behaviour between samples subjected to the two treatments (A and IC treatment). Due to the qualitative similarity between the different materials studied, only one PE, namely 7006 is used to illustrate the features of this comparison.

Figure 17 shows that the two-stage form of the $T_{htp} - \log t$ plots of the IC systems (see *Figure 2*) are absent or at least less pronounced for the A systems. The almost complete elimination of the stage 1 crystallization for the A systems is due to the almost complete constancy in W_s with treatment time. The stage 1 crystallization which is very clearly observable for the IC samples occurs within a period of significantly changing W_s. For the A systems, the $T_{htp} - \log t$ lines of the different T_a approach each other at

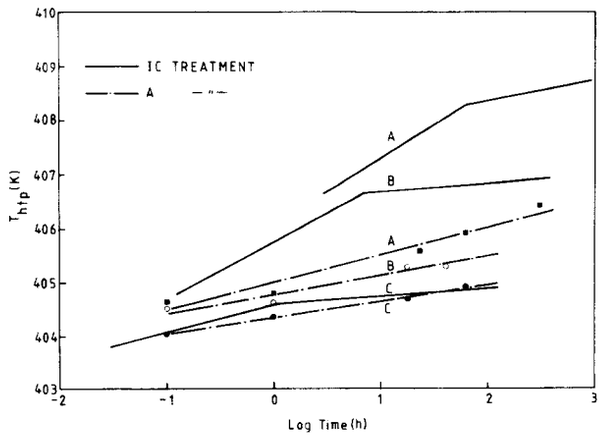

Figure 17 HT peak temperature T_{htp} plotted *versus* the logarithm of time (t) of isothermal treatment at T_c or T_a. The samples (7006) were either IC-treated (———) or A-treated (–·–·–) at three temperatures: A, 401.2 K; B, 398.2 K; C, 393.2 K

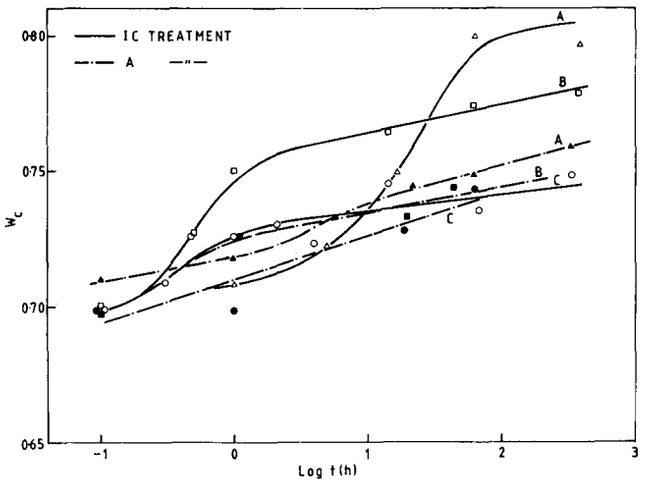

Figure 18 Crystallinity (W_c) at 300 K plotted *versus* the logarithm of time of isothermal treatment at T_c or at T_a. The samples (7006) were either IC-treated (———) or A-treated (–·–·–) at A: 401.2 K; △, IC; ▲, A. B: 398.2 K; □, IC; ■, A. C: 393.2 K; ○, IC; ●, A

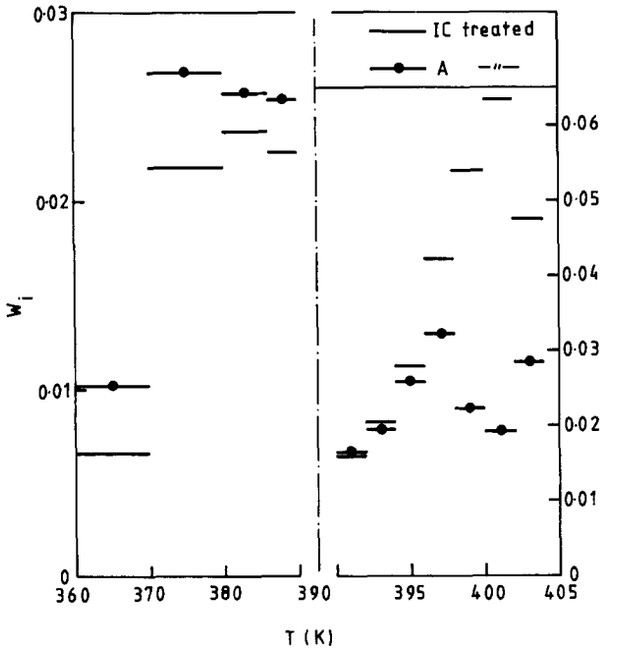

Figure 19 Comparison between systems treated according to IC (–) and A (–●–) regarding the LT peak. The mass fraction of the sample (7006, isothermally treated at 401.2 K for 300 h and finally cooled to 300 K at a rate of 1.25 K min^{-1}) melting within the denoted temperature ranges are shown

short times in a starting value of T_{htp}. This starting value is settled by the temperature range (from 396K and lower) at which crystallization occurs during the initial cooling phase of this treatment. The melting points of the crystals first formed in the IC samples are uniquely related to T_c. The difference in T_{htp} between the IC and A systems treated at 398.2 and 401.2K is to some extent due to this discrepancy in the melting points of the first formed crystals.

In *Figure 18* the smoothly shaped curves of the A samples contrast with the characteristic S-shaped curves of the IC samples. The absence of a period of strongly increasing W_c for the A samples is associated with the constancy of W_s for these systems (see *Figure 20*). The generally lower crystallinity of the A samples compared with the IC samples reflects the lower $W^0_{ns,c}$ values of the A systems. This is most probably a memory effect, assigned to the fact that crystals formed during the initial cooling stage of the A treatment are comparatively thin, i.e. of a relatively low melting point, with a relatively large fraction of amorphous material in between the crystals.

Figure 19 shows the occurrence of a lower W_{sl} value, a 5K lower temperature of the peak maximum, a smaller mass fraction of the sample melting in the high temperature region of the LT peak, and a slightly larger mass fraction melting in the low temperature region of this peak for the A sample than for the IC sample. The explanation to this discrepancy in melting behaviour has been given previously.

Figure 20 shows the lower equilibrium values of $W_{s,c}$ of the A samples compared with the IC systems. This difference becomes more pronounced at the higher temperatures of treatment. For the A samples, there is only a small change in $W_{s,c}$ with t_a. The times at which a constant $W_{s,c}$ is established seem to be approximately the same for samples of both the treatments. The only minor decrease in $W_{s,c}$ with treatment time for the A samples is due to the fact that a major part of the segregation is already completed after the initial cooling stage. Thus, the fraction of the sample present in the melt at the start of the annealing stage is only of a low concentration of molecules crystallizable at T_a. The difference in the $W_{sl,c}$ values between the IC and A systems is due to the fact that the crystals melting above T_a in the A samples contain molecules which by the IC treatment are non-crystallizable at a temperature equal to T_a.

CONCLUSIONS

The high temperature (HT) melting peak, appearing for samples isothermally crystallized at T_c from the melt, is associated with the melting of the material that has crystallized at T_c. Two stages are apparent, denoted, respectively, stage 1 and stage 2, in the development of the HT peak as a function of the crystallization time. Stage 1, featured by the rapid increase of the peak temperature T_{htp} with the crystallization time is associated with a phase of rapid crystallization at T_c. It is shown that the melting points of the newly formed crystals increases with increas-

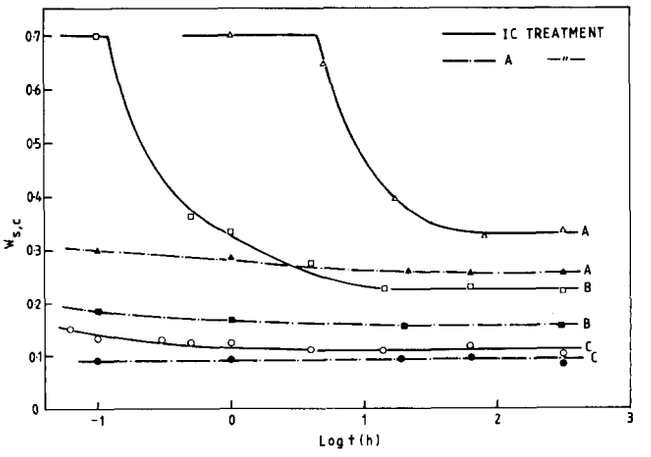

Figure 20 Mass fraction of the sample melting within the LT peak ($W_{s,c}$) plotted *versus* the logarithm of the time of isothermal treatment (at T_c or at T_a). The samples (7006) were either IC-treated (–) or A-treated (–·–) at A: 401.2 K; △, IC; ▲, A. B: 398.2 K; □, IC; ■, A. C: 393.2 K; ○, IC; ●, A

ing crystallization time. Stage 2, characterized by a much slower increase in T_{htp} with increasing crystallization time, appears after the establishment of a constant size of the low temperature melting peak. Evidence is provided for a slowly increasing crystallinity of the non-segregated component with time during this period. With the aid of the melting point—crystal thickness data by Illers and Hendus[37], under the assumption that all the increase of crystallinity is accomplished by the growth of the crystals along the chain axis, a relatively good fit is obtained between the set of data relating T_{htp} and crystallization time with the data relating crystallinity and crystallization time.

Data for the crystallinity (at 300K) as a function of time of crystallization for samples isothermally crystallized from the melt provide the basis for a model representing the material. The material is considered to consist of a non-segregated component (crystallized at T_c) and a segregated component (crystallized at temperatures below T_c), each of a certain crystallinity. The crystallinity of the non-segregated component increases with both T_c and the time of crystallization. It is shown that both these crystallinity values decrease with increasing degree of chain branching.

The low temperature (LT) melting peak, shown for samples isothermally crystallized (at T_c) from the melt, is associated with the material remaining uncrystallized at T_c. The development of the LT peak with the crystallization time proceeds through three stages: At the start there is a period with no isothermal crystallization, which is followed by a second stage of isothermal crystallization resulting in a decrease in both the size of the LT peak and the peak temperature, until finally constant values of these entities are approached. This fraction of the sample is truly uncrystallizable at T_c. A determination of this rejected, segregated material should take into account the differences in crystallinity between the segregated and the non-segregated components and also the surface melting of the crystals mainly melting in the HT peak. During the second stage it is observed that the mass fraction of the sample melting in the high temperature region of the LT peak decreases with crystallization time and that the mass fraction melting in the intermediate temperature range increases with crystallization time. These findings are consistent with the idea of a progressively decreasing crystallizability of the components of the remaining melt existing at T_c. An expected consequence of this fact is a reduction in the co-crystallization occurring between molecules of low and intermediate crystallizability. This seems to be the most plausible explanation for the data in the intermediate temperature range of the LT peak.

A method has been developed for studying segregation in samples crystallized during cooling at constant rate from the melt. There is evidence that the degree of co-crystallization between molecules of different ability to crystallize increases with increasing cooling rate. It is also shown that the co-crystallization predominantly involves molecules of crystallizability only slightly different from each other.

The development of T_{htp}, $W_{s,c}$ and W_c with the annealing time shows that a great deal of the segregation is already completed after the initial cooling stage of the A treatment. The occurrence of a significant amount of co-crystallization primarily involving molecules not significantly different from each other concerning their crystallizability, during the initial cooling in the A treatment is demonstrated.

ACKNOWLEDGEMENTS

The reported studies are parts of a research programme on mechanical properties of crystalline polymers sponsored by the National Swedish Board for Technical Development (STU). The authors wish to thank Mr S. Eklund at the Department for experimental assistance, Dr S. Holding at RAPRA of Great Britain for the g.p.c. analysis, and Unifos Kemi AB, Sweden for delivering the polyethylenes studied.

REFERENCES

1 Hawkins, S. W. and Smith, H. *J. Polym. Sci.* 1958, **28**, 341
2 Richards, R. B. *Trans. Faraday Soc.* 1946, **42**, 10
3 Konigsveld, R. and Pennings, A. J. *Rec. Trav. Chim.* 1964, **83**, 552
4 Prime, R. B. and Wunderlich, B. *J. Polym. Sci., Polym. Phys. Ed.* 1969, **7**, 2061
5 Sadler, D. M. *J. Polym. Sci., Polym. Phys. Ed.* 1971, **9**, 779
6 Anderson, F. R. *J. Appl. Phys.* 1964, **35**, 64
7 Anderson, F. R. *J. Polym. Sci., Polym. Symp.* 1965, **8**, 275
8 Keith, H. D. and Padden Jr, F. J. *J. Appl. Phys.* 1964, **35**, 1270
9 Keith, H. D. and Padden Jr, F. J. *J. Appl. Phys.* 1964, **35**, 1286
10 Moyer, J. D. and Ochs, R. J. *Science* 1963, **142**, 1316
11 Bank, M. I. and Krimm, S. *J. Polym. Sci., Polym. Lett.* 1970, **8**, 143
12 Harland, W. G., Khadr, M. M. and Peters, R. H. *Polymer* 1972, **13**, 13
13 Mehta, A. and Wunderlich, B. *Coll. Polym. Sci.* 1975, **253**, 193
14 Dlugosz, J., Fraser, G. V., Grubb, D. T., Keller, A., Odell, J. A. and Goggin, P. L. *Polymer* 1976, **17**, 471
15 Winram, M. M., Grubb, D. T. and Keller, A. *J. Mat. Sci.* 1978, **13**, 791
16 Smith, P. and St. John-Manley, R. *Macromolecules* 1979, **12**, 483
17 Martinez-Salazar, J. and Balta Calleja, F. J. *Polymer Bull.* 1980, **3**, 7
18 Gedde, U. W., Terselius, B. and Jansson, J-F. *Polym. Eng. Sci.* 1981, **21**, 172
19 Wunderlich, B. and Mehta, A. *J. Polym. Sci., Polym. Phys. Ed.* 1974, **12**, 255
20 Wunderlich, B. 'Macromolecular Physics', Vol. 2, Academic Press, New York, 1976, pp 88–105
21 Lindenmeyer, P. H., Beumer, H. and Hosemann, R. *Polym. Eng. Sci.* 1979, **19**, 51
22 Bryant, W. M. D. and Voter, R. C. *J. Am. Chem. Soc.* 1953, **75**, 6113
23 Preedy, J. E. and Wheeler, E. J. *Macromol. Chem.* 1977, **178**, 2461
24 Pella, E. and Nebuloni, M. *J. Thermal. Anal.* 1971, **3**, 229
25 Thermal Analysis Newsletter, No. 5, Perkin-Elmer Corporation, Norwalk, Conn.
26 Wunderlich, B. 'Techniques of Chemistry', Vol. 1: Physical Methods of Chemistry, Wiley-Interscience, New York, 1971, p 427
27 Gray, A. P. *Thermochim. Acta* 1970, **1**, 563
28 Richardson, M. J. *Plast. Rubber: Mat. Applications* 1976, **1**, 162
29 Blundell, D. J., Beckett, D. R. and Willcocks, P. H. *Polymer* 1981, **22**, 704
30 Wunderlich, B. and Baur, H. *Adv. Polymer. Sci.* 1970, **7**, 151
31 Wunderlich, B. 'Macromolecular Physics', Vol. 3, Academic Press, New York, 1980
32 Hellmuth, E. and Wunderlich, B. *J. Appl. Phys.* 1965, **36**, 3039
33 Weeks, J. J. *J. Res. Nat. Bur. Stand.—A* 1963, **67A**, 441
34 Kawai, T. *Kolloid-Z.* 1967, **229**, 116
35 Hoffman, J. and Weeks, J. J. *J. Res. Nat. Bur. Stand.—A* 1962, **66A**, 13
36 Varnell, W. D., Harrison, I. R. and Wang, J. I. *J. Polym. Sci., Polym. Phys. Ed.* 1981, **19**, 1579
37 Illers, K. H. and Hendus, H. *Macromol. Chem.* 1968, **113**, 1
38 Barham, P. J., Chivers, R. A., Jarvis, D. A., Martinez-Salazar, J. and Keller, A. *J. Polym. Sci., Polym. Lett.* 1981, **19**, 539
39 Hoffman, J. D. *Soc. Plastics Eng. Trans.* 1964, **4**, 315
40 Gedde, U. W., Eklund, S. and Jansson, J-F. *Polymer* 1983, **24**, 1532
41 Bares, V. and Wunderlich, B. *J. Polym. Sci., Polym. Phys. Ed.* 1973, **11**, 397